



Molecular Crystals and Liquid Crystals Science and Technology. Section A. Molecular Crystals and Liquid Crystals

Publication details, including instructions for authors and
subscription information:

<http://www.tandfonline.com/loi/gmcl19>

Numerical Calculations of Electroclinic Effect: Dynamic Response of Molecular Tilt and Dielectric Constant

Munehiro Kimura^a, Shigetsugu Okamoto^{a b}, Masataka Yamada^a,
Tadashi Akahane^a & Shunsuke Kobayashi^{a c}

^a Department of Electrical Engineering, Faculty of Engineering,
Nagaoka University of Technology, Kamitomioka 1603, Nagaoka,
Niigata, 940-21, Japan

^b Central Research Lab., Sharp Co.

^c Department of Electronic and Information Engineering, Faculty of
Technology, Tokyo University of Agriculture and Technology, Koganei
2-24-16, Tokyo, 184, Japan

Version of record first published: 23 Sep 2006.

To cite this article: Munehiro Kimura, Shigetsugu Okamoto, Masataka Yamada, Tadashi Akahane & Shunsuke Kobayashi (1995): Numerical Calculations of Electroclinic Effect: Dynamic Response of Molecular Tilt and Dielectric Constant, Molecular Crystals and Liquid Crystals Science and Technology. Section A. Molecular Crystals and Liquid Crystals, 263:1, 189-198

To link to this article: <http://dx.doi.org/10.1080/10587259508033583>

PLEASE SCROLL DOWN FOR ARTICLE

Full terms and conditions of use: <http://www.tandfonline.com/page/terms-and-conditions>

This article may be used for research, teaching, and private study purposes. Any substantial or systematic reproduction, redistribution, reselling, loan, sub-licensing, systematic supply, or distribution in any form to anyone is expressly forbidden.

The publisher does not give any warranty express or implied or make any representation that the contents will be complete or accurate or up to date. The accuracy of any instructions, formulae, and drug doses should be independently verified with primary sources. The publisher shall not be liable for any loss, actions, claims, proceedings,

demand, or costs or damages whatsoever or howsoever caused arising directly or indirectly in connection with or arising out of the use of this material.

NUMERICAL CALCULATIONS OF ELECTROCLINIC EFFECT: DYNAMIC RESPONSE OF MOLECULAR TILT AND DIELECTRIC CONSTANT

Munehiro KIMURA, Shigetsugu OKAMOTO,¹ Masataka YAMADA,
Tadashi AKAHANE and Shunsuke KOBAYASHI²

Department of Electrical Engineering, Faculty of Engineering, Nagaoka University of
Technology,

Kamitomioka 1603, Nagaoka, Niigata 940-21 Japan

²Department of Electronic and Information Engineering, Faculty of Technology, Tokyo
University of Agriculture and Technology, Koganei 2-24-16, Tokyo 184 Japan

Abstract The dynamic responses of the molecular tilt and the dielectric constant of liquid crystal cells which exhibit the electroclinic effect (ECE) in the SmA phase were studied. The numerical simulation of the dynamic ECE responses on a basis of the Landau-type formula was proposed. From the numerical results, it was examined that the non-polar and/or polar surface anchoring strength affects the molecular reorientational distribution. ECE responses was found to be affected by the order of the phase transition. The numerical results were confirmed through comparison with the experimental results.

1 Introduction

The electroclinic effect (ECE) in the smectic phase, which has been firstly described by Garoff and Meyer as a pretransitional behavior,¹⁾ is known for the liquid crystal (LC) molecular tilting phenomenon and accompanied critical behavior. When an electric field is applied parallel to the smectic layer, field-induced-tilt can be observed, where the tilt angle depends on the magnitude of the applied field. Generally speaking, the system without external field in the SmA phase is treated as uniaxial and LC molecules rotate freely along the longitudinal molecular axis. When an electric field is applied, the electric dipoles of LC molecules tends to align parallel to the field, and the molecular rotation

¹Present address: Central Research Lab., Sharp Co.

along the longitudinal axis is biased, then the molecular tilt appears. This phenomenon is so-called electroclinic effect. Particularly, the response speed are excellently fast because of the soft mode response, which is much attractive capability for the flat panel display devices.

The static theoretical analysis for ECE in the SmA phase has been performed by many investigators on a basis of the Landau-type free energy as to the bulk properties.¹⁻⁴⁾ Particularly, Ch.Bahr and G.Heppke insisted that, the experimental measurements of the molecular tilt angle and the electric polarization for the first-order phase transition FLC sample demonstrated the different behavior to the second-order sample, which could be explained by the Landau-type equation.⁵⁾ They also described that the temperature dependence of the static dielectric constant of the first-order FLC sample under the DC bias field exhibited the different characteristics to the second-order FLC sample. Their explanation based on the Landau-type equation is consistent with the phase transition characteristics and the variation of the dielectric constant.

Those studies have discussed in regard to only the bulk property but, as a matter of course, the surface anchoring effect has been neglected. In fact, the surface anchoring energy seems to affect the bulk properties, hence the theoretical analysis should include the surface anchoring energy. Following the consideration of Surface-Stabilized Ferroelectric Liquid Crystal (SSFLC), when the anchoring strength is fairly strong, the molecular orientation can not be regarded as uniform throughout the cell. Such the deformation of the molecular orientation may generate the polarization electric field. Therefore, the electric field also can not be regarded as homogeneous throughout the cell. Previously, Akahane et al.,^{6,7)} presented the theoretical analysis of dynamic response for SSFLCs based on the continuum theory in the SmC* phase including the effect of surface anchoring, polarization electric field and dielectric anisotropy. As far as the authors know, however, this kind of the detailed analysis with regard to the ECE phenomena have not been given yet, still less the dynamic ECE response.

In the present work, the numerical simulation of the dynamic ECE responses on a basis of the Landau-type formula, which includes the surface anchoring effect, elastic effect and polarization electric field, is proposed. The comparison with the experimental results is also discussed.

2 Theoretical model

It is well known that the ECE can be understood by analyzing the Landau-type free energy formula.¹⁻⁵⁾ In order to investigate the molecular reorientation and the dielectric response, we performed the numerical calculation for the ECE phenomena. Firstly we represent the equations based on the Landau-type free

energy formula as follows:

$$f_{\text{Landau}} = f_0 + \frac{1}{2}A\theta^2 + \frac{1}{4}B\theta^4 + \frac{1}{6}C\theta^6 + \frac{1}{2}\chi_p^{-1}P^2 - \frac{1}{2}(\epsilon^0 + \epsilon^1\theta^2)E_Y^2 - PE_Y - c\theta P, \quad (1)$$

where P is the component of the average polarization due to the orientation of permanent dipoles parallel to the applied electric field E_Y . The polarization P and molecular tilt angle θ are treated as independent variables. ϵ^0 is the conventional dielectric constant without contribution from the permanent dipole, ϵ^1 is the coefficient of the dielectric energy term corresponding to the field-induced dielectric biaxiality. χ_p is a generalized susceptibility, and c is the piezoelectric coupling constant. $A = a(T - T_0)$, B and C are the Landau coefficient. E_Y is given by

$$E_Y = -\frac{d\phi}{dY} = -\phi_{,Y}, \quad (2)$$

where ϕ is the electric scalar potential. By setting the partial derivative of f_{Landau} with respect to P equals to zero ($\partial f/\partial P = 0$), P is given by

$$P = \chi_p(E_Y + c\theta). \quad (3)$$

Substitution of eq.(3) into eq.(1) leads to

$$f_{\text{Landau}} = -\frac{1}{2}(\chi_p + \epsilon^0)E_Y^2 - \chi_p c E_Y \theta + \frac{1}{2}(A - \chi_p c^2 - \epsilon^1 E_Y^2)\theta^2 + \frac{1}{4}B\theta^4 + \frac{1}{6}C\theta^6. \quad (4)$$

The elastic free energy density f_{elas} , which is conventionally used in the nematic deformation, is simply given by

$$f_{\text{elas}} = \frac{1}{2}K\left(\frac{d\theta}{dY}\right)^2, \quad (5)$$

where K is the elastic constant.

We assume that the surfaces of bounding plates are homogeneous and characterized by the surface anchoring energy per unit area f_s given by⁸⁾

$$\begin{aligned} f_s^0 &= U\theta_0 + \frac{1}{2}G\theta_0^2 \\ f_s^d &= -U\theta_d + \frac{1}{2}G\theta_d^2, \end{aligned} \quad (6)$$

where superscripts 0 and d indicate the values at the lower and the upper bounding plates, respectively. The first term represents polar anchoring effect, which originates from the interaction with the electric polarizability. The second term represents non-polar and in-plane tilt anchoring effect.

If we define

$$f_B = f_{\text{Landau}} + f_{\text{elas}} \quad (7)$$

$$f_S = f_s^0\delta(Y) + f_s^d\delta(Y - d), \quad (8)$$

the total energy per unit area of the cell is given by

$$F = \int_0^d (f_B + f_S) dY, \quad (9)$$

where, f_B is the bulk free energy density and f_S is related to the surface anchoring energy.

Introducing the viscosity coefficient λ corresponding to the soft mode response, the torque balance equation can be written as

$$\lambda \frac{\partial \theta}{\partial t} = - \frac{\delta F}{\delta \theta}. \quad (10)$$

From eq.(10), we obtain

$$\lambda \frac{\partial \theta}{\partial t} = - \frac{\partial f_B}{\partial \theta} + \frac{\partial}{\partial Y} \frac{\partial f_B}{\partial \theta_Y} \quad (\text{in the bulk}) \quad (11)$$

Here, we used the static approximation for the surface torque balance equation,^{9,6)} i.e., the molecular reorientation at the surface is driven by the director motion in the bulk, which is given by

$$\left(\frac{\partial f_B}{\partial \theta_Y} \right)_{Y=0} = \frac{\partial f_s^0}{\partial \theta_0} \quad (\text{at the lower substrate}) \quad (12)$$

$$\left(\frac{\partial f_B}{\partial \theta_Y} \right)_{Y=d} = - \frac{\partial f_s^d}{\partial \theta_d} \quad (\text{at the upper substrate}) \quad (13)$$

Substitutions of eq.(4), (5) and (6) into eq.(11)-(13) lead to

$$\lambda \frac{\partial \theta}{\partial t} = \chi_P c E_Y - (A - \chi_P c^2 - \epsilon^1 E_Y^2) \theta - B \theta^3 - C \theta^5 + K \frac{\partial^2 \theta}{\partial Y^2}, \quad (14)$$

$$K \left(\frac{\partial \theta}{\partial Y} \right)_{Y=0} = U + G \theta_0, \quad (15)$$

$$K \left(\frac{\partial \theta}{\partial Y} \right)_{Y=d} = U - G \theta_d, \quad (16)$$

where θ_0 and θ_d are the values at $Y = 0$ and $Y = d$, respectively.

The scalar potential ϕ is determined from $\delta F / \delta \phi = 0$, i.e.,

$$\frac{\partial}{\partial Y} \left(\frac{\partial f_B}{\partial \phi_Y} \right) - \frac{\partial f_B}{\partial \phi} = 0. \quad (17)$$

Substitution of eq.(4) into eq.(17) lead to

$$\frac{\partial}{\partial Y} \{ (\chi_P + \epsilon^0 + \epsilon^1 \theta^2) \frac{\partial \phi}{\partial Y} - \chi_P c \theta \} = 0. \quad (18)$$

In terms of the normalized quantities, eq.(18) can be written as

$$\frac{\partial}{\partial \zeta} \left\{ \left(\frac{\chi_P}{\epsilon^0} + \frac{\epsilon^1}{\epsilon^0} \theta^2 + 1 \right) \frac{\partial \phi^*}{\partial \zeta} - \theta \right\} = 0 \quad (19)$$

where

$$\phi^* = \frac{\epsilon^0}{\chi_p c d} \phi, \quad \zeta = \frac{Y}{d}. \quad (20)$$

By integrating eq.(19), we obtain

$$\{(\frac{\chi_p}{\epsilon^0} + \frac{\epsilon^1}{\epsilon^0} \theta^2 + 1) \frac{\partial \phi^*}{\partial \zeta} - \theta\} = C_{\text{int}}, \quad (21)$$

where C_{int} is an integral constant. Then, ϕ^* is given by

$$\phi^* = \int_0^\zeta \frac{\theta + C_{\text{int}}}{\frac{\chi_p}{\epsilon^0} + \frac{\epsilon^1}{\epsilon^0} \theta^2 + 1} d\zeta. \quad (22)$$

When the applied voltage is v , C_{int} can be determined from the relation

$$\begin{aligned} v^* &= \frac{\epsilon^0}{\chi_p c d} v = \int_0^1 \frac{\theta + C_{\text{int}}}{\frac{\chi_p}{\epsilon^0} + \frac{\epsilon^1}{\epsilon^0} \theta^2 + 1} d\zeta \\ &= \int_0^1 \frac{\theta}{\frac{\chi_p}{\epsilon^0} + \frac{\epsilon^1}{\epsilon^0} \theta^2 + 1} d\zeta + C_{\text{int}} \int_0^1 \frac{d\zeta}{\frac{\chi_p}{\epsilon^0} + \frac{\epsilon^1}{\epsilon^0} \theta^2 + 1}. \end{aligned} \quad (23)$$

Then, we can obtain ϕ_ζ^* by eq.(21). The dielectric constant of the cell $\bar{\epsilon}$ can also be obtained from the following equation,

$$\frac{1}{\bar{\epsilon}} = \int_0^d \frac{dY}{\chi_p + \epsilon^0 + \epsilon^1 \theta^2 + \frac{\partial \theta}{\partial E} \{\chi_p C + 2E \epsilon^1 \theta\}}. \quad (24)$$

Finally, in explicit form, the torque balance equation in the bulk is given by

$$\frac{\partial \theta}{\partial \tau} = -\Lambda \phi_\zeta^* - A' \theta + \Lambda \frac{\epsilon^1}{\epsilon^0} \theta (\phi_\zeta^*)^2 - B' \theta^3 - C' \theta^5 + \frac{\partial^2 \theta}{\partial \zeta^2}, \quad (25)$$

where

$$\tau = \left(\frac{K}{\lambda d^2} t \right), \quad \Lambda = \frac{(\chi_p c d)^2}{K \epsilon^0},$$

$$\begin{aligned} A' &= \frac{d^2}{K} (A - \chi_p c^2), \quad B' = \frac{d^2}{K} B, \\ C' &= \frac{d^2}{K} C. \end{aligned}$$

The torque balance equation at the upper and lower substrate are given by

$$\left(\frac{\partial \theta}{\partial \zeta} \right)_{\zeta=0} = U' + G' \theta_0, \quad (26)$$

$$\left(\frac{\partial \theta}{\partial \zeta} \right)_{\zeta=1} = U' - G' \theta_d, \quad (27)$$

where

$$U' = \frac{U d}{K}, \quad G' = \frac{G d}{K} \quad (28)$$

To solve the set of eqs.(25), (26), (27), (23) and (24) simultaneously, we resort to the conventional difference method for the space Y and the time t derivatives. Then we can study the dynamic response of the director motion and dielectric constant of the cell. The number of divisions along the Y -axis is 40. The parameters used in our calculations are as follows. Landau coefficient $A = 8 \times 10^4$ ($\text{Jm}^{-3}\text{K}^{-1}\text{rad}^{-2}$), $C = 6 \times 10^6$ ($\text{Jm}^{-3}\text{K}^{-1}\text{rad}^{-6}$). Since the coefficient B depends on the order of the SmA-SmC* phase transition, we assumed $B = -1 \times 10^6$ ($\text{Jm}^{-3}\text{K}^{-1}\text{rad}^{-4}$) in the case of first order phase transition type and $B = 1 \times 10^6$ ($\text{Jm}^{-3}\text{K}^{-1}\text{rad}^{-4}$) in the case of second order type, respectively. The generalized susceptibility $\chi_p = 1 \times 10^{-10}$ (F/m), the piezoelectric coupling constant $c = 5.6 \times 10^7$ (V/m), elastic constant $K = 1.0 \times 10^{-10}$ (N), and the conventional dielectric coefficient $\epsilon^0 = 5 \times 10^{-11}$ (F/m). Here, the dielectric biaxiality ϵ^1 was neglected. Because the principal origin of the ECE is not the electronic polarization, but the polarization P due to the orientation of the permanent dipoles, thus the effect of dielectric biaxiality seems to be small. The cell thickness $d=2$ (μm), the viscosity coefficient $\lambda=5 \times 10^{-2}$ ($\text{N}\cdot\text{sec}/\text{m}^2$). The applied triangular wave voltage was assumed to be 20(Vp-p), 4 (kHz).

3 Numerical results

3.1 The surface effect on molecular reorientation

Figure 1 shows the example of the dynamic simulation of the molecular reorientational distributions under a triangular wave voltage. Here the anchoring strength was assumed to be weak such that $G = 1 \times 10^{-6}$ (N/m) and $U = 0$ (N/m). The coefficient B was assumed to be $B = -1 \times 10^6$ ($\text{Jm}^{-3}\text{K}^{-1}\text{rad}^{-4}$) corresponding to the first order phase transition. The meshed figure represents the uniform reorientational distribution which is in agreement with the conventional ECE response in whole the period. It suggests that this simulation based on the Landau-type equations is appropriate for studying the dynamic molecular

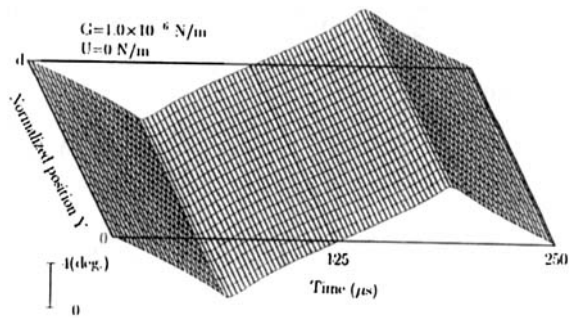


Figure 1 Examples of numerical simulations of dynamic molecular reorientations under the triangular wave voltage ($V=10$ V, $f=4$ kHz). The anchoring strength was assumed to be weak such that $G = 1 \times 10^{-5}$ (N/m) and $U = 0$ (N/m).

motions.

Fig.2 is the result when the non-polar anchoring strength G is 1×10^{-3} (N/m). The polar anchoring strength U is also neglected. In Fig.2, it is recognized that, when the applied voltage takes its maximum value, the molecular tilt angle near the surface are smaller than that in the bulk. This is because the molecule near the surface are unable to tilt freely since the molecules are anchored strongly by the orientational surface.

Figure 3 shows the effects of the polar anchoring strength on the molecular tilt. Where the polar anchoring strength U is 1×10^{-4} (N/m), and the non-polar anchoring strength G is 1×10^{-4} (N/m). In Fig.3, the molecules near the surface are tilted spontaneously even when the applied voltage is zero-crossed. And in whole the period, the molecules near the both surface are more tilted than that in the bulk. Eq.(6) indicates that the spontaneous molecular tilt causes the surface energy lower owing to the existence of the polar anchoring energy. Therefore, the molecular orientation exhibits S -like orientation. Chen *et al.* reported an experimental investigation of similar surface-twisted orientation of FLC as a surface-electroclinic effect.¹¹⁾ This surface-electroclinic effect seems to have some relationship to surface polar anchoring.

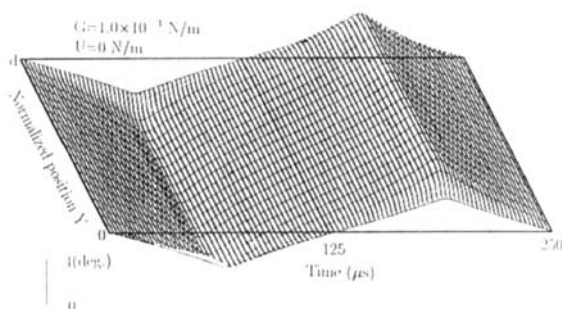


Figure 2 Numerical simulations of dynamic molecular reorientations under the triangular wave voltage ($V=10$ V, $f=4$ kHz), where the non-polar anchoring strength was assumed to be $G = 1 \times 10^{-3}$ (N/m) and $U = 0$ (N/m).

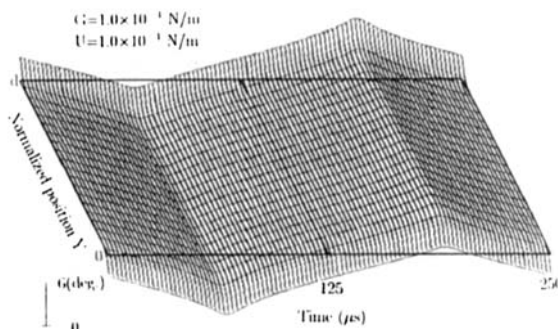


Figure 3 Numerical simulations of dynamic molecular reorientations under the triangular wave voltage ($V=10$ V, $f=4$ kHz), where the polar anchoring strength U is 1×10^{-4} (N/m), and the non-polar anchoring strength G is 1×10^{-4} (N/m).

3.2 The order of the phase transition

Figure 4 shows the example of the dynamic simulation of the dielectric constant under a triangular wave voltage. Where the anchoring parameter is the

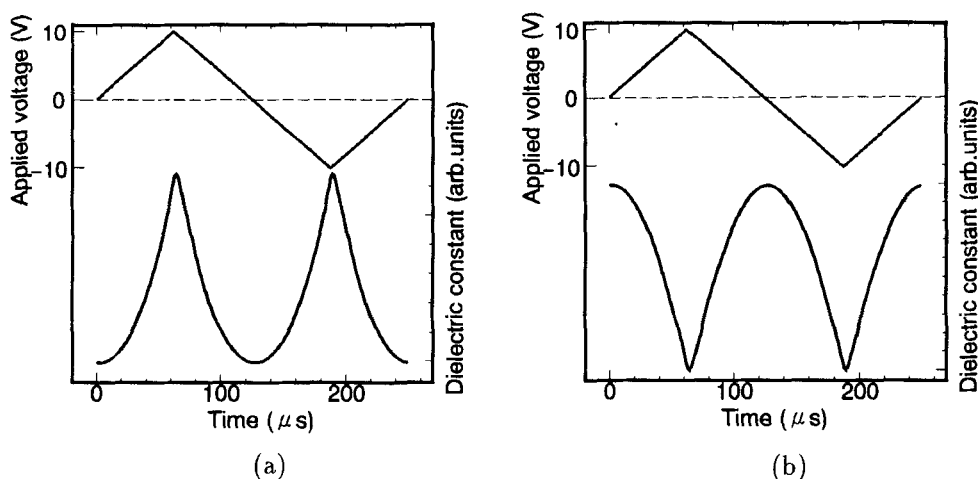


Figure 4 Numerical simulation of the dielectric constant responses; (a) in the case of the first-order phase transition, (b) in the case of the second-order phase transition.

same as Fig.1 for considering the weak anchoring. In order to investigate the effect of the order of the phase transition, the coefficient B were $B = -1 \times 10^6$ ($\text{Jm}^{-3}\text{K}^{-1}\text{rad}^{-4}$) corresponding to the first-order phase transition (as shown in Fig.4(a)), $B = 1 \times 10^6$ ($\text{Jm}^{-3}\text{K}^{-1}\text{rad}^{-4}$) corresponding to the second-order phase transition (as shown in Fig.4(b)), respectively. In the case of the first-order phase transition (Fig.4(a)), the dielectric constant increases with increasing the applied voltage. On the other hand, in the case of the second-order phase transition (Fig.4(b)), the dielectric constant decreases with increasing the applied voltage. It suggests that the variation of the dielectric constant under the applied electric field depends on the order of the phase transition. In regard to the theoretical discussion for the static characteristics, Ch.Bahr And G.Heppke have discussed the effect of the order of the phase transition on the electric displacement,⁵⁾ our result is consistent with their conclusion.

To verify the numerical results, the dynamic responses of the dielectric constant of the ECE samples were measured as shown in Fig.5. The samples used were antiferroelectric liquid crystals (R)-4-(1-trifluoromethylheptyloxy-carbonyl)-phenyl 4-(5-dodecyloxy-pyrimidin-2-yl)benzoate¹²⁾ (TFMHPDOPB) and (R)-4-(1-methylheptyloxy-carbonyl)phenyl 4'-octyloxybiphenyl-4-carboxylate¹³⁾ (MHPOBC), which exhibit a strong ECE in the SmA phase.^{14, 15)} The sample was filled and aligned in the sandwich type cell, whose inner surface were coated with polyimide and were rubbed unidirectionally. The cell thickness was about $2 \mu\text{m}$. The electrooptic (EO) response was measured under the crossed polarizers, where the incident polarizer was set parallel to the rubbing direction. The dynamic response of the dielectric constant of the LC sample cell was measured by using a system for measuring the transitional dielectric constant.¹⁶⁾

The dynamic responses of the dielectric constant and the optical response exhibiting the ECE in the SmA phase were shown in Fig.5. The experiments

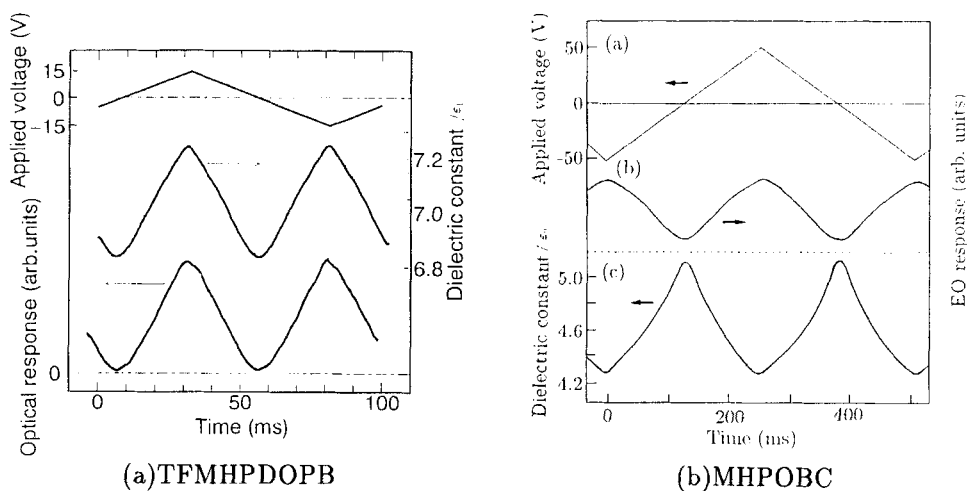


Figure 5 The response of the optical response and the dielectric constant for the ECE sample cells; (a)TFMHPDOPB, (b)MHPOBC.

were carried out at the temperature which is about 2°C above the SmA-SmC_A^* (or SmA-SmC_o^*) phase transition temperature. Fig.5(a) shows the results of the TFMHPDOPB whose order of the phase transition is first order.¹²⁾ It is clearly recognized that the dielectric constant increases with increasing the applied voltage, which is similar to the experimental result as shown in Fig.4(a). In contrast to TFMHPDOPB, in the case of the MHPOBC whose order of the phase transition is second order,¹⁷⁾ the dielectric constant decreases with increasing the applied voltage as shown in Fig.5(b), our experimental result is also the same as the numerical simulation.

4 Conclusion

The dynamic simulation of ECE phenomena, which was based on the Landau-type free energy formula and included the surface anchoring effect, elastic effect and polarization electric field, was proposed. The numerical results demonstrated the remarkable effect of the non-polar and/or polar surface anchoring strength on the molecular reorientation. It was also found that the dynamic response of the dielectric constant depended on the order of the phase transition. This numerical examination agreed with our experimental results qualitatively. Detailed researches on the effect of the surface effect and phase transition behaviors are now in progress and will be presented in the near future.

Acknowledgement

The authors would like to thank TOYO Corp. for helpful encouragement. We also would like to thank Mitsubishi Petrochemical Co.Ltd. and Chisso Co.Ltd.

for providing the LC materials.

References

- [1] S. Garoff and R. B. Meyer: Phys. Rev. **38** L848 (1977).
- [2] S. A. Pikin and V. L. Indenbom: Sov. Phys. USP **21** 487 (1978).
- [3] Y. B. Yang, N. Nakamura and S. Kobayashi: Jpn. J. Appl. Phys. **30** L612 (1991).
- [4] M. Glogarová, Ch. Destrade, J. P. Marcerou, J. J. Bonvent and H. T. Nguyen: Ferroelectrics **121** 285 (1991).
- [5] Ch. Bahr and G. Heppke: Phys. Rev. A **41** 4335 (1990).
- [6] T. Akahane, N. Nihei and K. Itoh: Jpn. J. Appl. Phys. **32** 5041 (1993).
- [7] T. Anabuki, T. Sakonjuh, M. Kimura and T. Akahane: Ferroelectrics **149** 21 (1993).
- [8] Y. B. Yang, T. Bang, A. Mochizuki and S. Kobayashi: Ferroelectrics **121** 113 (1991).
- [9] P. G. Amaya, M. A. Handchy and N. A. Clark: Opt.Eng. **23** 261 (1984).
- [10] R. C. Jones: J. Appl. Phys. **32** L486 (1942).
- [11] W. Chen, Y. Ouchi, T. Moses, Y. R. Shen and K. H. Yang: Phys. Rev. Lett **68** (1992) 1547.
- [12] S. Inui, S. Kawano, M. Saito, H. Iwane, Y. Takanishi, K. Hiraoka, Y. Ouchi, H. Takezoe and A. Fukuda: Jpn. J. Appl. Phys. **29** L987 (1990).
- [13] K. Furukawa, K. Terashima, M. Ichihashi, S. Satoh, K. Miyazawa and T. Inukai: Ferroelectrics **85** 451 (1988).
- [14] S. Nishiyama, Y. Ouchi, H. Takezoe and A. Fukuda: Jpn. J. Appl. Phys. **26** L1787 (1987).
- [15] M. Kimura, S. Okamoto, T. Akahane and S. Kobayashi: Ferroelectrics **147** (1994) 305.
- [16] M. Kimura, H. Maeda, M. Yoshida, A. Mochizuki and S. Kobayashi: Rev. Sci. Instrum. **62** 1609 (1991).
- [17] K.Hiraoka: personal communications.